

## **Free Vibrations of Circular Arches with Variable Cross-Section Considering Shear Deformation and Rotatory Inertia**

Sang Jin Oh<sup>†1)</sup>, Byoung Koo Lee<sup>†2)</sup> and In Won Lee<sup>†2)</sup>

<sup>†</sup> *Department of Civil Engineering, Wonkwang University, Iksan, Junbuk 570-749, Korea*

<sup>‡</sup> *Department of Civil Engineering, KAIST, Taejon 305-701, Korea*

### **ABSTRACT**

The differential equations governing free, in-plane vibrations of circular arches with variable cross-sections are derived and solved numerically to obtain frequencies. The effects of shear deformation, rotatory inertia and axial deformation are taken into account. The lowest four natural frequencies are calculated for quadratic arches with clamped-clamped and hinged-hinged end constraints.

### **INTRODUCTION**

The problem of the free vibration of arches has become a subject of interest for many investigators due to its importance in many practical applications. More than 300 articles studying free vibrations of arches are cited by Chidamparam and Leissa (1993). In spite of the fact that many papers deal with in-plane vibrations of arches there is a very limited number of studies available on the free vibration of arches with variable cross-section based on the Timoshenko beam theory in which both shear deformation and rotatory inertia are taken into account.

The main purpose of this paper is to present both the fundamental and some higher free vibration frequencies for linearly elastic circular arches with variable cross-section. Taking into account the effects of shear deformation, rotatory inertia and axial deformation, the differential equations for in-plane vibration are derived and solved numerically for quadratic arches with three types of rectangular section.

- 1) Post-Doctoral Fellow
- 2) Professor

# MATHEMATICAL MODEL

Consider the circular arch with variable cross-section, symmetric about the crown as shown in Figure 1(a). Shown in Figure 1(a) are the positive directions of radial and tangential displacements,  $w$  and  $v$ , and positive directions of the rotation angle  $\psi$  of the cross section at point  $\phi$ . The area moments of inertia of cross-section at  $\phi$ , at the crown of arch and at the left/right end are denoted as  $I$ ,  $I_c$  and  $I_e$ , respectively. The cross-sectional areas at  $\phi$  and at the crown of arch are denoted as  $A$  and  $A_c$ , respectively. The abscissa  $Z$  is measured from at any point of arch  $\phi$  to the arch vertical center line and the angle between the arch axis and the horizontal is  $\theta$ . The angle between the arch axis and the horizontal at the left end is  $\theta_e$  which is equal to half the subtended angle, or  $\alpha/2$ .

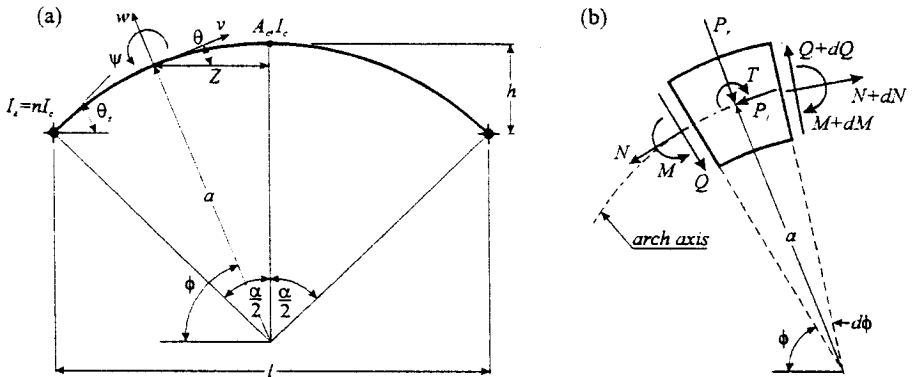


Figure 1. (a) Arch geometry; (b) Loads on an arch element.

The quantities  $A$  and  $I$  are expressed in the form

$$A = A_c F, \quad I = I_c H, \tag{1,2}$$

where both  $F$  and  $H$  are the functions of the single variable  $\phi$ .

The three equations for "dynamic equilibrium" of the arch element shown in Figure 1(b) are

$$N' + Q - aP_r = 0, \quad Q' - N - aP_t = 0, \quad a^{-1}M' - Q + T = 0, \tag{3-5}$$

where  $N$  is the axial force,  $Q$  is the shear force,  $M$  is the bending moment,  $P_r$  is the radial inertia force,  $P_t$  is the tangential inertia force,  $T$  is the rotatory inertia couple, and  $(\prime) = d/d\phi$ .

The bending moment, normal force and shear force with inclusion of the effects of rotatory inertia, shear deformation and axial deformation, are given by Henrych (1981), as

$$M = -EIa^{-1}\psi' = -EI_cHa^{-1}\psi', \tag{6}$$

$$N = EAa^{-1}(v' + w) + EIa^{-2}\psi' = EA_cFa^{-1}(v' + w) + EI_cHa^{-2}\psi', \tag{7}$$

$$Q = kAG\beta = kAGa^{-1}(w' - v - a\psi) = kA_cFGa^{-1}(w' - v - a\psi), \quad (8)$$

where  $E$  is the Young's modulus,  $G$  is the shear modulus,  $k$  is the shape factor of cross-section, and  $\beta$  is the angular deformation due to shear.

The arch is assumed to be in harmonic motion, or each displacement component is proportional to  $\sin(\omega t)$ , where  $\omega$  is the angular frequency and  $t$  is time. The inertia loadings are then

$$P_r = -\gamma A \omega^2 w = -\gamma A_c F \omega^2 w, \quad P_t = -\gamma A \omega^2 v = -\gamma A_c F \omega^2 v, \quad T = -\gamma I \omega^2 \psi = -\gamma I_c H \omega^2 \psi, \quad (9-11)$$

where  $\gamma$  is mass density of arch material.

To facilitate the numerical studies, the following non-dimensional system variables are defined:

$$f = h/l, \quad s = l/\sqrt{I_c/A_c}, \quad \mu = kG/E, \quad \rho = a/l, \quad (12-15)$$

$$\delta = w/l, \quad \eta = v/l, \quad C_i = \omega_i l^2 \sqrt{\gamma A_c / (EI_c)}. \quad (16-18)$$

When equations (6)-(11) together with equations (12)-(18) are used in equations (3)-(5), the results are

$$\delta'' = -F^{-1}F'\delta' + \mu^{-1}(1 - \rho^2 s^{-2} C_i^2)\delta + (1 + \mu^{-1})\eta' + F^{-1}F'\eta + (\rho + \rho^{-1}\mu^{-1}s^{-2}F^{-1}H)\psi' + \rho F^{-1}F'\psi, \quad (19)$$

$$\eta'' = -F^{-1}F'\eta' + (\mu - \rho^2 s^{-2} C_i^2)\eta - (1 + \mu)\delta' - F^{-1}F'\delta - \rho^{-1}s^{-2}F^{-1}H\psi'' - \rho^{-1}s^{-2}F^{-1}H'\psi' - \rho\mu\psi, \quad (20)$$

$$\psi'' = -H^{-1}H'\psi' + (\rho^2\mu s^2 FH^{-1} - \rho^2 s^{-2} C_i^2)\psi - \rho\mu s^2 FH^{-1}\delta' + \rho\mu s^2 FH^{-1}\eta. \quad (21)$$

From Figure 1(a), the span length  $l$  can be written as

$$l = 2(a - h)\tan(\alpha/2) = 2\sqrt{a^2 - (a - h)^2}. \quad (22)$$

With equations (12), (15) and (22),  $\rho$  and  $\alpha$  are calculated:

$$\rho = (4f^2 + 1)/(8f), \quad \alpha = 2\tan^{-1}\left[4f/(1 - 4f^2)\right]. \quad (23,24)$$

The shape functions  $F$  and  $H$  contained in equations (19)-(21) are now defined. Of the two basic classes of arched members, prime and quadratic (Leontovich 1969), the quadratic arch considered more economical in bridge construction is adopted here. A quadratic arch is defined as an arch whose moment of inertia of cross-section varies in accordance with the quadratic equation:

$$I = \frac{I_c}{\cos\theta \left[ 1 - \left( 1 - \frac{I_c}{I_e \cos\theta_e} \right) \left( \frac{2Z}{l} \right)^2 \right]} \quad (25)$$

The terms of  $\theta$  and  $2Z/l$  in above equation can be expressed in the variable  $\phi$  as follows.

$$\theta = \pi/2 - \phi, \quad 2Z/l = \cos\phi/\sin(\alpha/2). \quad (26,27)$$

A new non-dimensional parameter is defined as the ratio of  $I_e$  and  $I_c$ :

$$n = I_e/I_c. \quad (28)$$

When equations (26)-(28) and  $\theta_e = \alpha/2$  are substituted into equation (25) and the equations (2) and (25) are combined, the function of  $H$  can be expressed in terms of the variable  $\phi$ . The result is

$$H = 1/\left[ \sin\phi(1 + B\cos^2\phi) \right], \quad (29)$$

where

$$B = \frac{1}{\sin^2(\alpha/2)} \left[ \frac{1}{n\cos(\alpha/2)} - 1 \right]. \quad (30)$$

When equation (29) are differentiated once and twice, the results are

$$H' = H^2 \cos\phi(2B - 3B\cos^2\phi - 1), \quad H'' = 2H'^2 H^{-1} + H^2 \sin\phi(9B\cos^2\phi - 2B + 1). \quad (31,32)$$

The function  $F$  is defined for the three rectangular sections. The functions  $F$  and  $F'$  for rectangular section are expressed in the form

$$F = H^e, \quad F' = eH^{e-1}H'. \quad (33,34)$$

In equations (33) and (34) the values of  $e$  for depth, breadth and square tapers are 1/3, 1 and 1/2, respectively.

For the clamped-clamped beam, the boundary conditions at the ends are

$$\delta = 0, \quad \eta = 0, \quad \psi = 0. \quad (35a-c)$$

For the hinged-hinged beam, the boundary conditions at the ends are

$$\delta = 0, \quad \eta = 0, \quad \psi' = 0, \quad (36a-c)$$

where the last condition assures that the bending moment  $M$  given by equation (6) is zero.

Table 1. Comparisons of results between this study and reference (uniform section; clamped-clamped arch;  $\mu=0.327$ )

<i>i</i>	$f=0.134$				$f=0.289$			
	$s=20$		$s=100$		$s=34.64$		$s=173.2$	
	Irie <i>et al.</i>	This study	Irie <i>et al.</i>	This study	Irie <i>et al.</i>	This study	Irie <i>et al.</i>	This study
1	23.70	24.11	52.78	52.97	37.71*	32.10	35.37	35.34
2	38.73	39.85	75.98	76.19	45.51	45.99	69.72	69.78
3	62.35	63.71	117.8	118.6	73.89	75.75	127.1	127.4
4	69.97	73.67	170.8	173.0	91.14	93.30	184.2	184.9

Table 2. Frequency parameter  $C_i$  for clamped-clamped arches ( $\mu=0.3$ )

<i>f</i>	<i>s</i>	<i>n</i>	Depth taper				Breadth taper				Square taper				
			<i>i</i> =1	<i>i</i> =2	<i>i</i> =3	<i>i</i> =4	<i>i</i> =1	<i>i</i> =2	<i>i</i> =3	<i>i</i> =4	<i>i</i> =1	<i>i</i> =2	<i>i</i> =3	<i>i</i> =4	
0.1	20	uniform	22.12	41.59	63.52	74.34									
		3	25.24	45.91	67.67	78.57	26.06	47.18	75.45	79.44	25.48	46.33	69.60	78.88	
		7	27.02	48.41	69.90	81.12	28.31	50.99	81.39	83.86	27.42	49.28	72.82	82.04	
	100	uniform	56.13	64.16	116.2	180.7									
		3	66.45	67.70	131.4	203.5	63.30	71.40	123.1	190.5	65.69	68.69	129.4	200.4	
		7	69.39	73.21	141.6	217.8	68.95	74.25	130.3	200.1	70.75	72.21	138.9	213.8	
0.25	20	uniform	29.09	29.72	60.97	61.13									
		3	31.59	33.82	64.88	65.29	33.49	34.83	64.22	72.52	32.10	34.17	64.81	67.07	
		7	33.28	36.63	67.59	68.03	35.98	38.84	68.05	79.94	34.06	37.45	67.96	71.00	
	100	uniform	39.47	73.70	136.8	146.3									
		3	48.17	85.60	152.3	156.6	45.45	83.54	145.0	154.3	47.51	85.32	152.8	153.9	
		7	55.07	93.53	156.8	170.9	50.77	90.74	152.6	158.6	54.06	93.45	157.3	166.8	
0.4	20	uniform	19.42	29.08	48.46	52.24									
		3	22.06	30.46	51.30	54.87	22.87	32.21	51.84	59.13	22.29	30.93	51.49	55.98	
		7	25.19	32.84	53.66	58.04	26.24	36.84	51.84	66.15	25.64	33.93	53.45	60.26	
	100	uniform	24.30	50.38	92.53	133.9									
		3	28.80	56.70	102.5	144.4	28.51	56.09	99.86	144.0	28.73	56.58	101.9	144.5	
		7	35.02	66.31	116.9	158.2	32.34	61.91	104.2	150.1	34.39	65.45	114.0	157.8	

## NUMERICAL METHOD AND RESULTS

Based on the above analysis, a general FORTRAN computer program was written to calculate the frequency parameters  $C_i$ . The numerical methods described by Lee and Wilson (1989) and Wilson *et al.* (1994) were used to solve the differential equations (19)-(21), subject to the end constraint equations (35) or (36). The clamped-clamped and hinged-hinged end constraints were considered for the three cross-sectional shapes, for given parameters  $f$ ,  $s$ ,  $n$  and  $\mu$ . In this study, the four lowest values of  $C_i$  were calculated and the numerical results are shown in Tables 1-3. To show the validity of the present analysis, the numerical results for clamped-clamped arches with uniform cross-section are compared with transfer matrix solutions obtained by Irie *et al.* (1983) in Table 1. The good agreement is observed, except 37.71\* in Table 1. However, 37.71\* should be 31.71 (Kang *et al.* 1995).

In Tables 2 and 3 are given the lowest four frequency parameters for the arches with clamped-clamped and hinged-hinged end constraints. From these results, it can be seen that the  $C_i$  values increase as the value of  $n$  increases, with several exceptions for hinged-hinged arches with breadth taper. The  $C_i$  values always increase as the value of  $s$  increases. As one might expect,

Table 3. Frequency parameter  $C_i$  for hinged-hinged arches ( $\mu=0.3$ )

$f$	$s$	$n$	Depth taper				Breadth taper				Square taper			
			$i=1$	$i=2$	$i=3$	$i=4$	$i=1$	$i=2$	$i=3$	$i=4$	$i=1$	$i=2$	$i=3$	$i=4$
0.1	20	uniform	16.44	31.91	63.23	66.09								
		3	17.05	34.29	67.31	70.12	17.49	32.53	66.98	75.28	17.18	33.91	69.30	69.43
		7	17.37	35.43	69.50	72.24	17.87	32.79	67.85	81.24	17.55	34.90	71.40	72.49
	100	uniform	35.86	63.63	90.23	145.7								
		3	38.67	67.70	95.08	159.6	35.71	71.21	86.58	146.3	37.94	68.67	92.98	156.3
		7	39.63	69.32	97.23	165.5	35.37	74.21	84.54	146.2	38.59	70.73	94.15	160.7
0.25	20	uniform	21.21	28.31	52.30	61.06								
		3	23.29	29.73	55.71	65.13	21.97	31.58	51.58	72.53	23.01	30.26	54.73	66.99
		7	24.46	30.58	57.92	67.82	22.13	32.78	51.72	79.66	24.00	31.34	56.52	70.92
	100	uniform	23.76	57.14	109.8	146.2								
		3	26.27	64.81	122.9	151.5	24.04	60.33	111.4	154.3	25.72	63.81	120.0	152.4
		7	27.45	69.01	130.3	154.0	23.83	60.98	111.9	158.3	26.57	67.30	125.8	155.4
0.4	20	uniform	12.32	28.32	42.15	51.69								
		3	12.89	29.92	43.02	54.39	12.74	31.01	42.11	57.00	12.86	30.24	42.82	55.22
		7	14.38	32.76	44.24	57.87	13.03	34.71	39.62	60.26	14.10	33.68	42.92	59.53
	100	uniform	13.44	37.34	73.54	116.5								
		3	13.99	39.65	77.95	124.0	13.63	38.42	74.55	119.4	13.91	39.36	77.14	123.0
		7	15.75	45.41	87.98	139.2	13.83	39.85	75.71	121.0	15.29	44.16	84.97	135.2

it is apparent that the natural frequencies increase as the end constraint changes from hinged-hinged to clamped-clamped, other parameters remaining the same.

## CONCLUSIONS

The differential equations for in-plane free vibrations of circular arches with variable cross-sections, including the effects of shear deformation, rotatory inertia and axial deformation, were derived and solved numerically to obtain frequencies. The lowest four natural frequencies were calculated for quadratic arches with clamped-clamped and hinged-hinged end constraints. The effects of the taper type,  $f$ ,  $s$  and  $n$  on  $C_i$  were investigated.

## REFERENCES

- Chidamparam, P. and Leissa, A. W. (1993), "Vibrations of planar curved beams, rings and arches," *Applied Mechanics Reviews* **46**, 467-483.
- Henrych, J. (1981), *The Dynamics of Arches and Frames*, Elsevier.
- Irie, T., Yamada, G. and Tanaka, K. (1983), "Natural frequencies of in-plane vibration of arcs," *Journal of Applied Mechanics* **50**, 449-452.
- Kang, K., Bert, C. W. and Striz, A. G. (1995), "Vibration analysis of shear deformable circular arches by the differential quadrature method," *Journal of Sound and Vibration* **181**, 353-360.
- Lee, B. K. and Wilson, J. F. (1989), "Free vibrations of arches with variable curvature," *Journal of Sound and Vibration* **136**, 75-89.
- Leontovich, V. (1969), *Frames and Arches*, McGraw-Hill.
- Wilson, J. F., Lee, B. K. and Oh, S. J. (1994), "Free vibrations of circular arches with variable cross-section," *Structural Engineering and Mechanics* **2**, 345-357.